RSC Advances

ROYAL SOCIETY OF CHEMISTRY

www.rsc.org/advances

Cite this: DOI: 10.1039/c0xx00000x

www.rsc.org/xxxxxx

Paper

Liposomal nanohybrid cerasomes for controlled insulin release

Yushen Jin,[a,b] Yanyan Li,[b] Hongjie Pan,[b] and Zhifei Dai*[a]

Received (in XXX, XXX) Xth XXXXXXXXX 20XX, Accepted Xth XXXXXXXXX 20XX
DOI: 10.1039/b000000x

This study reported a facile fabrication of a reproducible and injectable cerasomal insulin formulation by encapsulating insulin into cerasomes via one-step construction. Notably, a wide range of the insulin release profiles were achieved by altering vesicle composition through incorporating phospholipid of DPPC into cerasomes, and the mixed cerasomes showed excellent storage stability when the percentage content of DPPC was lower than 50%. It was found that the subcutaneous administration of the insulin-loaded cerasomes resulted in a reduction of blood glucose levels in a rat model of type I diabetes and the hypoglycemic effect was found to composition-dependent. The use of cerasomes significantly improved glucose tolerance from 6 hours (free insulin) to more than 16 hours (insulin-loaded cerasomes). Moreover, the insulin-loaded cerasomes displayed a prolonged and stable glucose-lowering profile over a period of over 12 hours compared with the insulin-loaded liposomes. These findings demonstrate that cerasomes have good potential for the use of an effective controlled release delivery system of insulin as well as other proteins with short half-life time.

Introduction

In recent decades, more and more people suffer from diabetes mellitus[1,2] , which affects the quality of human life. Insulin is a very important protein which plays a crucial role in carbohydrate and fat metabolism.[3] Therefore, insulin has been emerged as a principal therapy to treat certain forms of diabetes mellitus. Insulin-dependent diabetes mellitus (IDDM, Type I diabetes) is a metabolic disorder which is caused by the destruction of insulin-secreting β-cells of the pancreatic islets of Langerhans.[1,4] However, there are still some difficulties in the delivery of insulin, such as poor permeability because of its high molecular weight[5] , lack of lipophilicity[6-8] short half-life of 5-20 min as a result of the inactivation and digestion by various proteolytic enzymes. Multiple doses are needed to maintain a constant plasma concentration for a good therapeutic response. Current dosage regimes of insulin that maintain low serum glucose levels comprise up four subcutaneous injections per day, causing uncomfortableness and painfulness.[9] In addition, it has lots of side-effects, such as impairment of the membrane barrier or some uncertain effects and often results in hypoglycemia if the insulin dosage is too high.[10] In order to reduce the injection frequency and maintain normoglycemia in a longer time, people developed various long acting insulin formulations, which have a peak effect occurring after 8-10 hours and its duration of action may be 12-16 hours.

To prolong the bioactivity of insulin ***in vivo***, a variety of nanomaterials, such as liposomes,[11] poly (lactide-co-glycolide) acid (PLGA),[8,12-14] chitosan,[15-18] carbon nanotubes,[19] gold nanoparticles[3,20,21] and polypeptides,[22,23] have been tailored for intracellular protein delivery with some success. Among numerous carriers, liposomes have attracted intensive interests due to their good biocompatibility, capability to encapsulate a wide range of drugs, biodegradability and controlled drug release properties. However, the well-known instability of the liposomes in biological medium may limit their wide applications in biomedicine.[24] Hence, many efforts have been exerted to improve the stability of liposomal vesicles such as PEGylated liposomes.[25] However, the liposomal preparations containing PEGylated phospholipids may cause skin toxicity generally known as "Hand-Foot syndrome".

To overcome general problems associated with current liposome technology, a hybrid liposomal cerasome was fabricated using self-assembly and sol-gel strategy.[26] Its atomic layer of polyorganosiloxane surface imparts higher morphological stability than conventional liposomes and its liposomal bilayer structure reduces the overall rigidity and density greatly compared to silica nanoparticles so biomimetic cerasome has drawn much attention as a novel drug delivery system.[27-29]

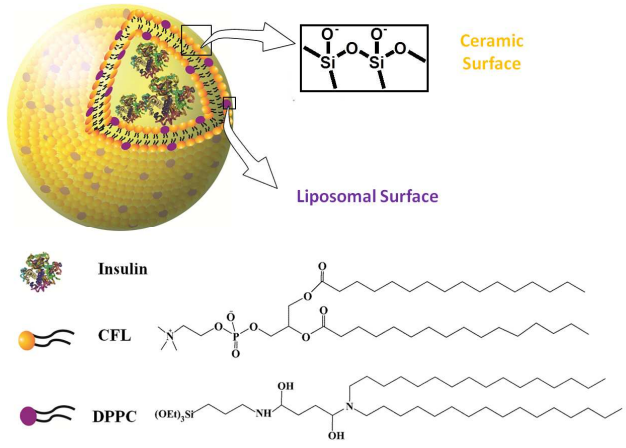

Fig.1. Structures of the insulin-loaded mixed cerasomes (ILMCs).

In the present report, insulin was loaded into cerasomes according to the Bangham method[30] in combination of self-assembly and sol-gel process, and the release rate of insulin from cerasomes was modulated by incorporating dipalmitoylphosphatidylcholine (DPPC) in cerasome (**Fig.1**). Consequently, a wide range of release profiles are achieved by altering the molar ratios of the cerasome-forming lipid (CFL) and phospholipids. The physical-chemical properties of the vesicles were studied. Meanwhile, the encapsulation capacity, drug leakage and ***in vitro*** biocompatibility of the vesicles were also investigated. In addition, the bioactivity of the insulin-loaded vesicles ***in vivo*** also assessed by measuring blood glucose levels of the diabetics rats and the results indicated that the cerasomes could be a promising carrier to promote the absorption of therapeutic protein drugs after administration subcutaneously.

Materials and Methods

Materials

The CFL of N-[N-(3-Triethoxysilyl)propylsuccinamoyl]-dihexadecylamine was synthesized according to the reported method.[31] Streptozotocin (STZ; MW: 265.2, Sigma) and insulin (28.8U/mg; MW 5807.69, Xuzhou Wanbang Biopharmacy Company) are commercially available products. DPPC was obtained from Nanjing Kangsente Chemical Engineering Co. Cholesterol (Chol) was from Shanghai Advanced Vehicle Technology Pharmaceutical Ltd. Fetal bovine serum (FBS) was from Zhejiang Tianhang Biological Technology Co. 3-(4,5-Dimethylthiazol-2-yl)-2,5-diphenyl tetrazolium bromide (MTT) was from AMRESCO Inc. RPMI-1640 was from Thermo Fisher Scientific Inc. Dimethyl sulfoxide (DMSO) was purchased from Sigma-Aldrich. Dialysis membrane (molecular weight cut-off *MWCO:* 1.2-1.4 kDa, California, USA) was from Spectrum Laboratories Inc. Deionized (DI) water (resistivity 18.2 MΩ/cm^2) was obtained by purification of house-distilled water with a Milli-Q Gradient System. The other chemicals were all of analytical grade. Unless otherwise stated, all reagents and chemicals were commercially obtained and used without further purification.

Fabrication of mixed cerasomes and insulin-loaded mixed cerasomes

Mixed cerasomes (MCs) and insulin-loaded mixed cerasomes (ILMCs) were prepared according to the Bangham method[30] in combination of sol-gel reaction with self-assembly process (as **Fig.1** shown). The alkoxysilyl head of the water-insoluble CFL was hydrolyzed to enable cerasome self-assembly,[28] since it was not charged and could not form a liposomal bilayer.[27,31] The hydrolysis of CFL was performed by addition of HCl (pH=3 diluted by ethanol, 1 mL/3mg CFL) as an acid catalyst, followed by incubation for an appropriate time at 40 ^{o}C,[26] which would made its alkoxysilyl head hydrolyzed into Si-OH. Then, chloroform and different amount of DPPC were added to the obtained sol and dried in a rotary evaporator to form a thin film layer, followed by drying overnight in vacuum. The obtained lipid film was hydrated in water or insulin solution (a 1:10 insulin/lipid molar ratio was used) at 40 ^{o}C for 30 min, and sonicated in water for 5 min to form multilamellar vesicles followed by 3 min ultrasonication with a probe-type sonicator to reduce and homogenize the vesicles size distribution. Then, the ILMCs were centrifuged at 30 000 rpm for 45 min to remove the unloaded insulin. The MCs and ILMCs suspension was stored in tight containers at room temperature for 24 h to form polysioxane networks on the surface of the vesicles by Si-OH condensation. Then, the vesicle suspensions were stored at 4 ^{o}C for further experiments. Conventional liposomes made up of DPPC and Chol with a molar ratio about 4:1 and insulin-loaded liposomes (ILLs) were prepared as a control study using the same process. However, conventional liposomes and ILLs were not ultrasonicated using the probe-type sonicator because of their poor stabilities.

Characterization of the vesicles

Vesicle size and zeta potential

Size distribution measurements on all vesicles solutions were performed with a 90Plus/BI-MAS dynamic light scattering (DLS) analyzer (Brookhaven Instruments Co., USA). The instrument uses a helium laser at a wavelength of 632.8 nm and detection at an angle of 90°. All measurements were performed in a temperature controlled chamber at 25 ^{o}C. The intensity-weighted size distribution was obtained and the measurements were repeated six times per sample. Zeta potential of all vesicles was also analyzed in the same Brookhaven instruments performing at least six runs per sample.

Transmission electron microscopic (TEM) measurements

TEM measurements of the vesicles with different formulation were operated at an accelerating voltage of 100 kV (Hitachi H-7650, Tokyo, Japan). Samples for TEM analysis were prepared by placing drops of the vesicle solutions on carbon-coated TEM copper grids. The vesicle solutions were allowed to be adsorbed on to the copper grids for 1 min, after which the extra solution was removed using blotting paper. Then, the mixtures were negatively stained with 2% (w/v) uranyl acetate, and thirty seconds later, the extra dye was removed using blotting paper.

Fourier transform infrared (FTIR) spectroscopy

FTIR spectra of all samples were recorded on a Varian Resolution Fourier transform infrared spectrophotometer (Varian FTS 3100, USA) at a resolution of 4 cm^{-1} in the range of 400 cm^{-1} ~ 4000 cm^{-1} region at 2 mm/s at room temperature with nitrogen gas. For comparison, an FTIR spectrum of pure insulin was also recorded. The resultant spectra were smoothed with a seven-point Savitsky Golay smooth function to remove the noise.[32-34]

In vitro stability of the vesicles

The capability to prevent leakage of aqueous contents and keep the structural integrity of the bilayer of the vesicles were analyzed by *UV-vis* spectrophotometer and DLS, respectively. The stability of the ILMCs were investigated in comparison with that of the conventional liposomes.

The drug leakage of different vesicle formulations was determined in the presence of phosphate buffer solution (PBS, pH7.4) at 4 ^{o}C. Briefly, 100 μL of different vesicles were diluted up to 1 mL with PBS followed by incubation at 4 ^{o}C for different time and their effects on encapsulation efficiency was measured. The vesicles were centrifuged at 30 000 rpm for 45 min, supernatant was collected and analyzed by *UV-vis* spectrophotometer. The results were reported as mean ± SD (n = 4). The drug loading content (DLC) and encapsulation efficiency

(EE) were evaluated by the method reported in our previous study.[5,27,29]

$$DLC(\%) = \frac{W_{drug\,in\,vesicles}}{W_{vesicles}} \times 100\% \quad \textbf{Eqs.(1)}$$

$$EE(\%) = \frac{W_{drug\,in\,vesicles}}{W_{feeding\,drug}} \times 100\% \quad \textbf{Eqs.(2)}$$

The size distribution of the vesicles at different storage time and different storage temperature was analyzed for the structural stability of the bilayer. Briefly, vesicles at a lipid concentration of 1.25 mg/mL were stored at 37 ^{o}C or 4 ^{o}C for 90 days. At predetermined time, the diameter of the vesicles was evaluated by DLS and the measurements were repeated at least six times each sample.

In vitro release properties of the insulin-loaded vesicles

The release properties of insulin from various vesicles were investigated using the dialysis method. Briefly, 1 mL of insulin-loaded vesicles suspensions were placed in dialysis bags and were suspended in 25 mL of PBS. The release media was incubated at 37 ± 0.1 ^{o}C with stirring. At specified time intervals, 1 mL of the sample was taken and the same volume of fresh media was added to maintain a constant volume. The amount of insulin release from insulin-loaded vesicles was estimated via *UV-vis* spectrophotometer without further treatment. All release tests were performed in quintuplicate, and the mean values were reported.

Cell culture and antiproliferative activity of various vesicles

Human umbilical vein endothelial cells (HUVECs) were grown and cultured in a 96-well plate at a density of 8×10^3 cells per well according to our previous protocol.[27] Cells were incubated with various vesicles at different concentrations for 24 h. Cell viability was measured by MTT assay according to the manufacturer suggested procedures. Cell viability was determined with the following equation:

$$Cell\,viability\,(\%) = \frac{A_{experiment} - A_{negative\,control}}{A_{positive\,control} - A_{negative\,control}} \times 100\% \quad \textbf{Eqs.(3)}$$

In the equation (3), the A value represents the absorbance intensity of each specimen at a wavelength of 492 nm.

In vivo studies of the insulin-loaded vesicles in diabetics rats

The male Wistar rats weighting 200 ± 20 g were obtained from Beijing Vital River Laboratories (Beijing, China) and acclimated for a period of two weeks under normal conditions with free access to food and water in the new environment before initiation of the experiments. Diabetes was induced by intraperitoneal injection of STZ (70 mg/kg) in a 0.1 mol/L citrate buffer at pH 4.5.[5,35,36] Rats were considered diabetic when the fasting blood glucose level was higher than 16.5 mmol/L about one week after STZ treatment. All animal procedures were in agreement with institutional animal use and care committee and carried out ethically and humanely.

The efficacy of the insulin-loaded vesicles for diabetes treatment was evaluated ***in vivo*** using STZ-induced adult diabetic rats. The blood glucose levels of rats were continuously tested for 2 days before administration by collecting blood from the tail vein and measuring using a Free Style Blood Glucose Meter (Yi Cheng, China) and the corresponding reagent paper. Then six diabetic rats fasted for 12 h were selected for each group administered with 0.9% saline, free insulin, ILLs, or ILMCs (10:0, 7:3, 1:1 or 3:7). A 1 mL amount of vesicles solution, free insulin solution or 0.9% saline solution was injected using a 1 mL syringe with a 19-gauge needle into the subcutaneous dorsum of rats (insulin dose: 100 IU/kg for vesicles or 5 IU/kg for free insulin). The glucose level of each rat was monitored over time. Furthermore, in order to estimate these hypoglycemic effects quantitatively, real time level of the plasma glucose (*RL*%) were calculated according to the following equation:

$$RL(\%) = \frac{G_t}{G_0} \times 100\% \quad \textbf{Eqs. (4)}$$

Where G_t refers to the plasma glucose levels of the rats at t h after subcutaneous administration of the samples and G_0 refers to the fasting blood glucose level at zero-time (before administration of the samples).

Statistics

Each value was expressed as mean ± SD, from several separate experiments. The one-tailed Student's t-test (SPSS, Chicago, USA) was performed to analyze the data of the two groups. P values of 0.05 or less were considered significant, while values of 0.01 or less were considered very significant.

Results and Discussion

Preparation and characterization of various vesicles

Various vesicles of 164~241 nm in size were prepared by varying the molar ratios of CFL to DPPC using the thin film hydration method (**Table 1**). The particles size was evaluated by using DLS to be 164.5 ± 2.6 nm (ILLs), 241.2 ± 1.5 nm (ILMCs 10:0), 230.2 ± 3.3 nm (ILMCs 7:3), 205.7 ± 9.2 nm (ILMCs 5:5) and 175.3 ± 11.6 nm (ILMCs 3:7), respectively. The vesicle size increased with the molar ratio of CFL to DPPC. The polydispersity indexes (PI) were all less than 0.3 for all vesicles, indicating that the vesicles have a certain homogeneity in size in DI water. In DI water the vesicles of ILLs displayed low zeta potential since DPPC and Chol are electrically neutral. In contrast, the cerasomes possessed a zeta potential of -37.27 ± 0.96 mV because of the negatively charged hydroxyl groups of polysioxane networks formed on their surface. Compared with ILLs, the higher negative charges on the surface of ILMCs could prevent aggregation, thus enhance the morphological stability of vesicles. Interestingly, the zeta potentials of ILMCs monotonically increased as the content of DPPC increased. However, the average zeta potential of the ILMCs all decreased to nearly electrically neutral both in PBS (pH7.4) and RPMI-1640 containing 10% fetal bovine serum (FBS), indicating the potential applicability of this delivery system ***in vivo***. The EEs of vesicles with different formulations were evaluated to be 49.52 ± 1.89% (ILLs), 45.93 ± 1.76% (ILMCs 10:0), 46.27 ± 2.41% (ILMCs 7:3), 47.03 ± 5.82% (ILMCs 5:5) and 47.58 ± 3.24% (ILMCs 3:7), and the DLCs were 0.27 ± 0.01 g/g (ILLs), 0.26 ± 0.01 g/g (ILMCs 10:0), 0.26 ± 0.01 g/g (ILMCs7:3), 0.26 ± 0.03 g/g (ILMCs 5:5) and 0.26 ± 0.02 g/g (ILMCs3:7), respectively. The obtained vesicles were also examined by TEM.

As seen in **Fig.2**, all vesicles show spherical shape and sizes below 240 nm, which are in accordance with the DLS measurements.

To further confirm the formation of polysioxane networks on the surface of the cerasomes and the successfully encapsulation of insulin into cerasomes, samples were analyzed by FTIR spectroscopy (**Fig.3**). As shown in **Fig.3**, a board and strong peak at around 1080 cm^{-1} was contributed to the overlapped stretching vibration of P=O bond and Si-O-Si bonds, which is a good indicator of the formation of polysioxane networks. As seen in **Fig.3**, peaks at 1487 cm^{-1} due to C=C aromatic stretching vibration seen in insulin are shifted to 1485 cm^{-1} in the ILMCs (10:0). Otherwise, peaks at 1569 cm^{-1} due to the amide N-H band observed in the case of ILMCs (10:0) were red shifted to a small extent compared to those of insulin at 1574 cm^{-1} . In the case of insulin alone, an intense peak is observed at 1659 cm^{-1}, which is attributed to the amide □stretching vibration and typical for α-helix conformation. This peak is also seen in the case of ILMCs (10:0) at 1652 cm^{-1} though less intense due to interactions with the cerasomes indicating that the conformation of insulin is relatively similar in the vesicles. All these results indicated that the insulin was successfully entrapped by the vesicles.

Table1. Characterization of insulin-loaded vesicles

Type of vesicles	Diameter(nm)	PI	Zeta potential (mV) in DI water	DLC (g/g)	EE (%)
ILMCs (10:0)	241.2±1.5	0.14	-37.27±0.96	0.26±0.01	45.93±1.76
ILMCs (7:3)	230.2±3.3	0.19	-34.63±1.27	0.26±0.01	46.27±2.41
ILMCs (5:5)	205.7±9.2	0.27	-25.42±0.48	0.26±0.03	47.03±5.82
ILMCs (3:7)	175.3±11.6	0.32	-13.51±2.70	0.26±0.02	47.58±3.24
ILLs	164.5±2.6	0.16	-4.92±0.34	0.27±0.01	49.52±1.89

PI: polydispersity index; DLC: drug loading content; EE: encapsulation efficiency

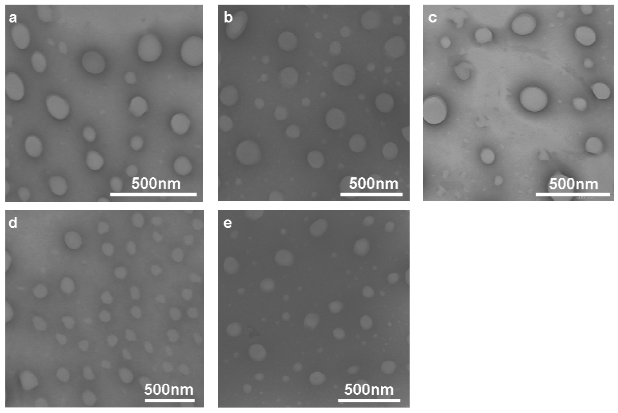

Fig.2. TEM images of ILLs (a), ILMCs (10:0) (b), ILMCs (7:3) (c), ILMCs (1:1) (d) and ILMCs (3:7) (e).

In vitro stability of the vesicles

It is well known that vesicle size plays a key role on the tissue distribution and clearance of drug-loaded vesicles. Also, the drug leakage is a critical parameter that affects the therapeutic efficacy of the content. Therefore, it is critical to retain the requisite size of vesicles and the amount of encapsulated drug during the process of storage. The morphological stability of various vesicles was examined by analyzing the diameter of the vesicles by DLS measurements over 3 months of storage at 4 °C or 37 °C, respectively. As shown in **Fig.4,** the size of ILMCs (10:0) remained unchanged due to the highly stable polysiloxane networks and negative charges on their surfaces. In contrast, ILLs increased from less than 200 nm in size to 607.4 nm and 1310.2 nm after 3 months of storage in aqueous solution at 4 °C and 37 °C, respectively. The increase in ILLs size was attributed to the lower zeta potential and membrane fluidity of the liposomes, which could induce aggregation and/or fusion of the nanovesicles. The introduction of 30% DPPC into cerasomes did not affect the long-term storage stability of the ILMCs at 4 °C and 37 °C. Moreover, ILMCs containing 50% DPPC were also stable in the period of storage at 4 °C. Nevertheless, when the content of DPPC increased to 70%, the ILMCs became much unstable at 4 °C or 37 °C due to the lower degree of polymerization of silanol group on the surface of the vesicles. Over 90 days of storage, the diameter of ILMCs with 70% DPPC increased from 175.3 nm to 521.8 and 795.2 nm at 4 °C and 37 °C, respectively. The rapid increase in vesicle size suggests that the storage stability of the nanovesicles was temperature-dependent and the MCs containing high DPPC content were not suitable for long-term storage.

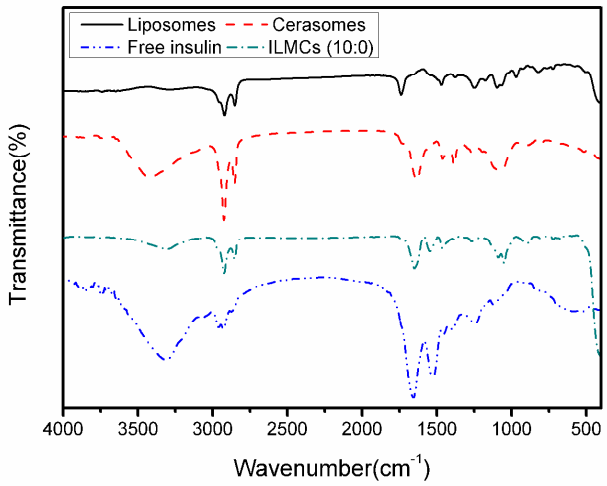

Fig.3. FTIR spectroscopic analysis of the formation of polysiloxane networks on the surface of the cerasomes and the encapsulation of insulin into cerasomes.

The drug leakage from ILLs and ILMCs in storage medium at 4 °C was also examined. As shown in **Fig.5**, there were only 8.0 ± 1.4% and 9.6 ± 2.1% of the drug payload released from ILMCs (10:0) and ILMCs (7:3) after 90 days storage, respectively, indicating the incorporation of 30% DPPC into cerasomes had

little effect on the storage stability of cerasomes. On the contrary, about 57.5 ± 3.1% of the initially loaded insulin was leaked from the ILLs, and about 27.5 ± 2.9% and 37.7 ± 1.5% of the insulin was leaked from ILMCs containing 50% and 70% DPPC over 90 days storage. It suggested that the leakage of insulin from various vesicles depended on the content of the incorporated DPPC. The stability of vesicles decreased with decreasing the molar ratio of CFL to DPPC. Therefore, higher content of DPPC in vesicles resulted in higher leakage loss of the loaded insulin during storage in solutions.

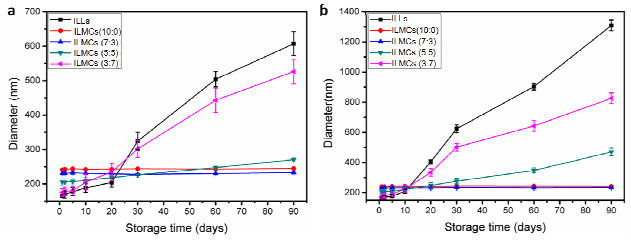

Fig.4. The hydrodynamic diameter (D_{hy}) of various vesicles after storage for 3 months at 4 °C (a) and 37 °C (b). Data shown as means ± SD (n = 5).

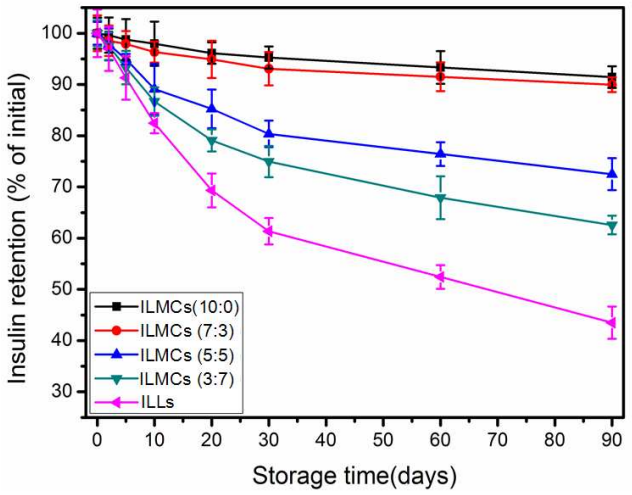

Fig.5. Retention of the encapsulated insulin in the ILLs (◂) and ILMCs (10:0■, 7:3●, 5:5▲, 3:7▼)) as a function of time. Data shown as means ± SD (n = 5).

In vitro drug release studies

To demonstrate how the vesicle composition affects the insulin release profiles, the ***in vitro*** insulin release from various vesicles was examined over a time period of experimental observation of 77 h. **Fig.6** showed the release profiles for the ILMCs compared to those of the ILLs and free insulin in PBS (pH7.4) at 37 °C. If there was no drug carrier, 87.3 ± 2.0% of insulin was released within 15 h. As expected, the insulin release from carriers was slower than that in the control solution. In the first 30 h, all the drug-loaded vesicles displayed a fast insulin release and the release was drastically slowed down in the next 30 h. For example, ILLs released 85.2 ± 2.9% insulin in the first 30 h with an additional release of less than 14.8 ± 1.6% in the next 47 h. Compared to the rapid insulin release from ILLs, ILMCs (10:0) only released 42.4 ± 3.0% insulin in the first 30 h and the total insulin release in 77 h was 62.8 ± 3.4%. Clearly, the accumulative release and release rates of insulin from the ILMCs increased as the content of DPPC increased. Specifically, the ILMCs containing 30%, 50% and 70% DPPC released 56.2 ± 3.4%, 68.1 ± 2.5%, and 74.5 ± 3.4% insulin in 30 h, respectively. The accumulative insulin release from the related ILMCs reached 71.2 ± 1.6%, 84.1 ± 2.5% and 91.1 ± 3.2% in 77 h.

The increased release rates and amounts of insulin from the MCs are likely attributed to the enhanced membrane permeability due to the introducing DPPC. The formation of siloxane networks may block the drug release channels, resulting slower release rate [29]. Nevertheless, lipid domains exist in the mixed cerasomes since the polymerizable nature of the CFL head group should cause phase separation,[37] which results in less stability. It is expected that the permeability of MCs to insulin can be modulated by varying DPPC contents. Indeed, we achieved a wide range of insulin release profiles by varying the molar ratio of CFL to DPPC in MCs. As a result, the engineering of MCs offers a strategy to modulate the insulin release profiles from liposomal cerasomes.

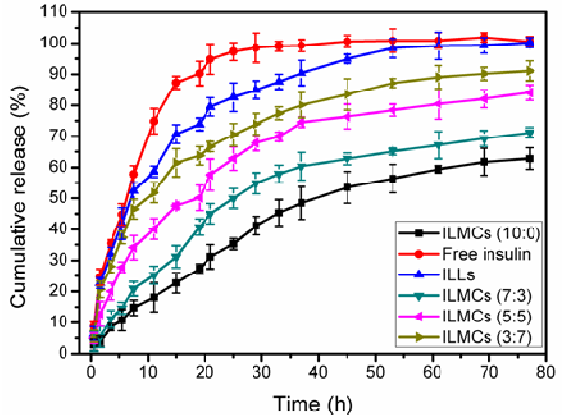

Fig.6. *In vitro* release of insulin from free insulin (●), ILLs (▲) and ILMCs(10:0■, 7:3▼,5:5◂, and 3:7▸) into the release medium at 37 °C.

Inhibitory effect of various vesicles on cell proliferation

The cytotoxicities of insulin-loaded vesicles were analyzed through incubated with HUVECs. No appreciable deduction in cell viability was observed when HUVECs were exposed to insulin-loaded vesicles at different lipid concentrations from 0.01 to to 1.0 mg/mL (**Fig.7**). In addition, no obvious difference in cell viability was observed among various vesicles. The results suggested that all these vesicles are highly biocompatible and are suitable for drug delivery.

In vivo studies of insulin-loaded vesicles in diabetics rats

The pharmacological efficacy of insulin ***in vivo*** of the insulin-loaded vesicles in type I diabetes was evaluated by measuring blood glucose levels (BGLs) of STZ-induced diabetes rats. The wistar rats whose BLG was higher than 16.5 mmol/L were used for further experiments. The STZ-induced diabetic rats were divided into seven groups and after fasting for 12 h, they were subcutaneously injected with different insulin-loaded vesicles at a dose of 100 IU/kg, 0.9% NaCl or free insulin at dose of 5 IU/kg. Because of a over dose of free insulin alone (higher

than 5 IU/kg) could cause hypoglycemic shock,[38,39] which would cause immediate death, in this study the free insulin were administrated at dose of 5 IU/kg. However, all the diabetes rats treated with insulin-loaded vesicles survived, which may be attributed to the sustained release of insulin from vesicles. In order to get a better effect, a relatively higher dose (100 IU/kg) of the insulin-loaded vesicles was used here, because different insulin doses provided very similar constants (dose-independent).[40]

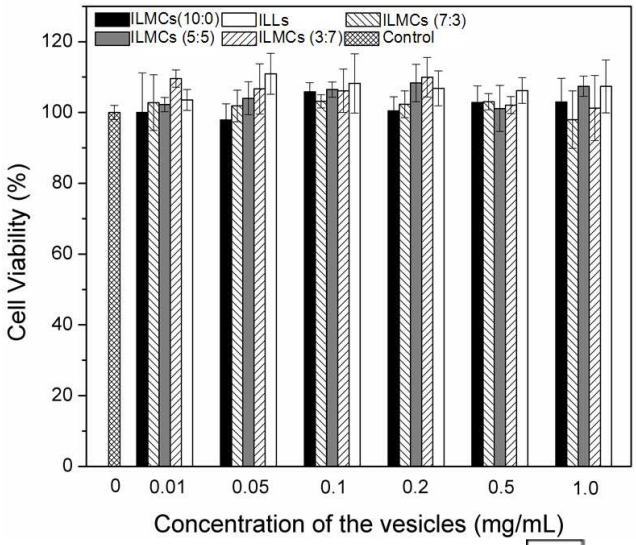

Fig.7. Anti-proliferative effect of ILLs( ), ILMCs(10:0 , 7:3 , 1:1 . 3:7) in HUVECs at different concentrations (n=3) after 24 h incubation.

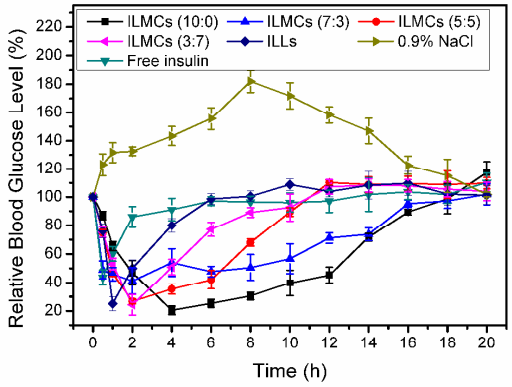

Fig.8. Hypoglycemic effect of insulin with different formulations to diabetes rats (mean ± SD) (free insulin▼, ILLs◆, 0.9%NaCl▶, ILMCs(10:0 ■, 7:3▲, 1:1●, 3:7◀)) .

Blood glucose level (BGLs) (% of initial value) verses time profiles following administration of different formulations is depicted in **Fig.8.** The BGLs of each animal group were closely monitored after administration at predetermined time and continuously recorded for 2 days. It was found that BGLs of rats injected with insulin-loaded vesicles quickly declined to a normoglycemic state (<11.1 mmol/L) within 1 h or 2 h. It was attributed to an initial burst release of the insulin from drug carriers due to the large concentration gradient between the blood and the drug carriers. The BGLs of the rats with ILMCs (7:3) or ILMCs (10:0) were then maintained in the normoglycemic range for up to 16 h and gradually increased afterward. In the absence of vesicles, the BGLs of rats with free insulin steadily increased back to a hyperglycemic state 6 h after injection. These results were in consistent with the releasing data above suggested that the insulin-loaded vesicles exert their prolonged glucose-lowering effect by decreasing the release rate of the insulin. However, the blank vesicles suspensions (data not shown) groups or 0.9% NaCl solution group did not display a noticeable decline in BGLs, indicating that the hypoglycemic effects were caused by the insulin instead of the drug carriers or the solvent. Somewhat of increase in BGLs above the baseline was observed, which may be attributed to the change of metabolisms and the increase of endogenous secretion of glucagon in the diabetic rats due to stress in the animals during blood sampling. The potential ***in vivo*** toxicity of insulin-loaded vesicles was evaluated by body weight loss. As seen in **Fig.9**, due to the easy access for food and water after fasting for 12 h, there was an apparent body weight increase in all seven groups after administration indicating that the insulin-loaded vesicles induced no systemic toxicity to the treated rats. It can also be used to explain the BGLs increase in the 0.9% NaCl control study. All these results suggested that the cerasomes can act as a ideal carrier for insulin delivery.

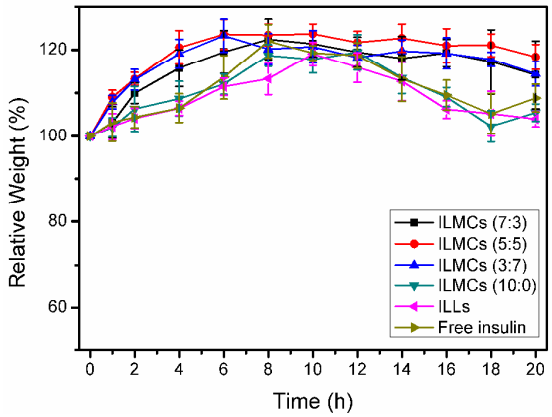

Fig.9. Body weights of rats at different time points after subcutaneous injection of different insulin formulations: ILLs(□), free insulin(▶) and ILMCs(10:0▼, 7:3■, 1:1●, 3:7▲).

Conclusions

A reproducible and injectable insulin formulation was constructed by loading insulin into nanohybrid cerasomes through thin-film hydrated method in combination of sol-gel reaction and self-assembly process. The ***in vitro*** experiments showed that the insulin-loaded cerasomes exhibited remarkably long-term storage stability, lower drug leakage, and more sustained release than conventional liposomes. Especially, the release profiles of insulin could be readily modulated by altering vesicle composition through DPPC incorporation. Most importantly, the ILMCs (10:0) showed a significant and prolonged hypoglycaemic effect, which lowered the blood glucose level of diabetic rats at insulin doses of 100 IU/kg up to 90% of their basal glucose level and kept for more than 16 h. In contrast, the blood glucose level of rats with free insulin and ILLs steadily increased back to a

hyperglycemic state after 6 h injection. The high long-term storage stability of cerasomes in solution over liposomes, together with their controllable sustained release, makes cerasomes a promising carrier for protein and peptide drug delivery. Further studies are underway.

Acknowledgments

This work was financially supported by the State Key Program of National Natural Science of China (no.81230036) , National High Technology Research and Development Program of China (no. 2013AA032201), National Natural Science Foundation of China (no. 21273014 and 81371580) and National Natural Science Foundation for Distinguished Young Scholars (no. 81225011).

Notes

[a]*Department of Biomedical Engineering, College of Engineering, Peking University, Beijing, 100871, China. E-mail: zhifei.dai@pku.edu.cn Homepage: http://bme.pku.edu.cn/~daizhifei*
[b]*Nanomedicine and Biosensor Laboratory, School of Life Science and Technology, Harbin Institute of Technology, Harbin 150080, China.*

References

1 K. K. Claudia R. Gordijo, Adam J. Shuhendler, Leonardo D. Bonifacio, Hui Yu Huang, Simon Chiang, Geoffrey A. Ozin, Adria Giacca and Xiao Yu Wu, *Adv Funct Mater*, 2011, **21**, 73.
2 M. May, in Scientific American Pathways-The Challenge of Changing Health-The changing science, business & experience of health, Scientific American, New York, 2010.
3 H. M. Joshi, D. R. Bhumkar, K. Joshi, V. Pokharkar and M. Sastry, *Langmuir*, 2006, **22**, 300.
4 B. O. Roep and T. I. Tree, Nature reviews, 2014, 10, 229.
5 J. Zheng, X. Yue, Z. Dai, Y. Wang, S. Liu and X. Yan, *Acta Biomater*, 2009, **5**, 1499.
6 F. Cardenas-Bailon, G. Osorio-Revilla and T. Gallardo-Velazquez, *J Microencapsul*, 2013, **30**, 409.
7 S. Soares, A. Costa and B. Sarmento, *Expert Opin Drug Deliv*, 2012, **9**, 1539.
8 N. Reix, A. Parat, E. Seyfritz, R. Van der Werf, V. Epure, N. Ebel, L. Danicher, E. Marchioni, N. Jeandidier, M. Pinget, Y. Frere and S. Sigrist, *Int J Pharm*, 2012, **437**, 213.
9 D. R. Owens, B. Zinman and G. B. Bolli, Lancet, 2001, 358, 739.
10 N. Jeandidier and S. Boivin, *Adv Drug Deliv Rev*, 1999, **35**, 179.
11 Z. H. Wu, Q. N. Ping, Y. Wei and J. M. Lai, *Acta Pharmacol Sin*, 2004, **25**, 966.
12 F. Ungaro, R. d'Emmanuele di Villa Bianca, C. Giovino, A. Miro, R. Sorrentino, F. Quaglia and M. I. La Rotonda, *J Control Release*, 2009, **135**, 25.
13 P. Fonte, F. Andrade, F. Araujo, C. Andrade, J. Neves and B. Sarmento, *Methods Enzymol*, 2012, **508**, 295.
14 S. Jain, V. V. Rathi, A. K. Jain, M. Das and C. Godugu, *Nanomedicine*, 2012, **7**, 1311.
15 Y. Zhang, W. Wei, P. Lv, L. Wang and G. Ma, *Eur J Pharm Biopharm*, 2011, **77**, 11-19.
16 S. Al-Qadi, A. Grenha, D. Carrion-Recio, B. Seijo and C. Remunan-Lopez, *J Control Release*, 2012, **157**, 383.
17 M. R. Avadi, A. M. Sadeghi, N. Mohammadpour, S. Abedin, F. Atyabi, R. Dinarvand and M. Rafiee-Tehrani, *Nanomedicine*, 2010, **6**, 58.
18 E. Lee, J. Lee and S. Jon, *Bioconjug Chem*, 2010, **21**, 1720.
19 A. Patel, K. Cholkar and A. K. Mitra, Ther Deliv, 2014, 5, 337.
20 D. R. Bhumkar, H. M. Joshi, M. Sastry and V. B. Pokharkar, *Pharm Res*, 2007, **24**, 1415.
21 H. J. Cho, J. Oh, M. K. Choo, J. I. Ha, Y. Park and H. J. Maeng, *Int J Biol Macromol*, 2014, **63**, 15.
22 Y. Shechter, M. Mironchik, S. Rubinraut, A. Saul, H. Tsubery and M. Fridkin, *Bioconjug Chem*, 2005, **16**, 913.
23 K. Thibaudeau, R. Leger, X. Huang, M. Robitaille, O. Quraishi, C. Soucy, N. Bousquet-Gagnon, P. van Wyk, V. Paradis, J. P. Castaigne and D. Bridon, *Bioconjug Chem*, 2005, **16**, 1000.
24 F. Frezard and C. Demicheli, *Expert Opin Drug Deliv*, 2010, **7**, 1343.
25 K. Iwanaga, S. Ono, K. Narioka, M. Kakemi, K. Morimoto, S. Yamashita, Y. Namba and N. Oku, *J Pharm Sci*, 1999, **88**, 248.
26 K. Katagiri, R. Hamasaki, K. Ariga and J. Kikuchi, *J Sol-Gel Sci Technol*, 2003, **26**, 393.
27 Y. Jin, X. Yue, Q. Zhang, X. Wu, Z. Cao and Z. Dai, *Acta Biomater*, 2012, **8**, 3372.
28 Z. Cao, Y. Ma, X. Yue, S. Li, Z. Dai and J. Kikuchi, *Chem Commun*, 2010, **46**, 5265.
29 Z. Cao, X. Yue, Y. Jin, X. Wu and Z. Dai, *Colloids Surf B*, 2012, **98**, 97.
30 A. D. Bangham, M. M. Standish and J. C. Watkins, *J Mol Biol*, 1965, **13**, 238.
31 K. Katagiri, M. Hashizume, K. Ariga, T. Terashima and J. Kikuchi, *Chemistry*, 2007, **13**, 5272.
32 B. Sarmento, D. C. Ferreira, L. Jorgensen and M. van de Weert, *Eur J Pharm Biopharm*, 2007, **65**, 10.
33 L. Jorgensen, C. Vermehren, S. Bjerregaard and S. Froekjaer, *Int J Pharm*, 2003, **254**, 7.
34 W. G. Dai and L. C. Dong, *Int J Pharm*, 2007, **336**, 58.
35 K. B. Chalasani, G. J. Russell-Jones, S. K. Yandrapu, P. V. Diwan and S. K. Jain, *J Control Release*, 2007, **117**, 421.
36 S. Lee, K. Kim, T. S. Kumar, J. Lee, S. K. Kim, D. Y. Lee, Y. K. Lee and Y. Byun, *Bioconjug Chem*, 2005, **16**, 615
37 M. Hashizume, I. Saeki, M. Otsuki, J. Kikuchi, J Sol-Gel Sci Techn, 2006, **40**, 227.
38 X. Y. Xiong, Y. P. Li, Z. L. Li, C. L. Zhou, K. C. Tam, Z. Y. Liu and G. X. Xie, *J Control Release*, 2007, **120**, 11.
39 A. Kim, M. O. Yun, Y. K. Oh, W. S. Ahn and C. K. Kim, *Int J Pharm*, 1999, **180**, 75.
40 M. Baudys, D. Letourneur, F. Liu, D. Mix, J. Jozefonvicz and S. W. Kim, *Bioconjug Chem*, 1998, **9**, 176.